Physics in Medicine & Biology

PAPER

Normalized glandular dose (DgN) coefficients from experimental mammographic x-ray spectra

To cite this article: Josilene C Santos *et al* 2019 *Phys. Med. Biol.* **64** 105010

IOP Publishing Phys. Med. Biol. 64 (2019) 105010 (15pp) https://doi.org/10.1088/1361-6560/ab171a

Physics in Medicine & Biology

IPEM Institute of Physics and Engineering in Medicine

PAPER

Normalized glandular dose (DgN) coefficients from experimental mammographic x-ray spectra

Josilene C Santos[1,4], Alessandra Tomal[2], Nestor de Barros[3] and Paulo R Costa[1]

[1] Instituto de Física da Universidade de São Paulo, São Paulo-SP, 05508-090, Brazil
[2] Instituto de Física Gleb Wataghin, IFGW-UNICAMP, Campinas-SP, 13083-859, Brazil
[3] Faculdade de Medicina da Universidade de São Paulo, São Paulo-SP, 05403900, Brazil
[4] Author to whom any correspondence should be addressed.

E-mail: josilene@usp.br

RECEIVED
28 November 2018

REVISED
23 March 2019

ACCEPTED FOR PUBLICATION
8 April 2019

PUBLISHED
10 May 2019

Keywords: mammography, normalized glandular dose coefficients, x-ray spectrometry, dosimetry

Abstract

Mean glandular dose is the quantity used for dosimetry in mammography and depends on breast-related characteristics, such as thickness and density, and on the x-ray spectrum used for breast imaging. This work aims to present an experimentally-based method to derive polyenergetic normalized glandular dose coefficients (DgN_p) from the spectral difference between x-ray spectra incident and transmitted through breast phantoms with glandular/adipose proportions of 30/70 and 50/50 and thicknesses up to 4.5 cm. The spectra were produced by a Mammomat 3000 Nova system using radiographic techniques commonly applied for imaging compressed breast thickness lower than 6 cm (Mo/Mo, Mo/Rh and W/Rh spectra at 26 and 28 kVp). DgN_p coefficients were compared with values estimated using Boones' method and data from breast images (DICOM Organ Dose and VolparaDose calculations). The DgN_p were also evaluated in layers into the phantoms (depth-DgN_p) using both x-ray spectra and thermoluminescent dosimeters (TLD-100). Maximum differences between DgN_p from the method presented in this study and results using Boone's method was 11%, with larger differences for Mo/Rh spectra in relation to the Mo/Mo. The DgN_p maximum differences to the coefficients obtained using patient images were 8.0%, for the DgN calculated using Volpara and 6.4% for the DgN from DICOM Organ Dose, for a 4.5 cm breast phantom with 30% glandularity. The DgN_p estimated from the depth-DgN_p distributions differ up to 5.2% to the coefficients obtained using the pair incident-transmitted spectra to calculate the DgN_p directly in the whole phantom. The depth-DgN_p distributions estimated with TLDs were consistent with the results observed using the experimental spectra, with maximum difference of 3.9%. In conclusion, polyenergetic x-ray spectrometry proved to be an applicable tool for research in dosimetry in mammography allowing spectral characterization. This approach can also be useful for investigation of the influence of x-ray spectra on glandular dose.

1. Introduction

Mammography is the reference technique used for early detection (screening) and diagnosis of breast cancer (Marmot *et al* 2012, Njor *et al* 2012). Since there is a risk of radiation-induced carcinogenesis associated this imaging procedure (Hendrick 2010, Pauwels *et al* 2016), the accurate determination of radiation dose delivered in mammography is essential for risk estimation, optimization procedures and for assessment of mammography systems (Dance *et al* 1999).

Mean glandular dose (MGD) is the accepted quantity by the scientific community and it is adopted by the mammography dosimetry protocols of several countries (ACR 1999, IAEA 2011, European Commission (EC) 2013, Gennaro *et al* 2018). This quantity depends on parameters related to the breast (glandularity and thickness) and to the x-ray spectrum (anode/filter combination, tube potential and half value layer) chosen for the imaging procedure. Given the impossibility to measure MGD directly, and due the complexity and individuality of each human breast, this quantity has generally been derived using Monte Carlo simulations (Dance 1990,

Boone 1999, 2002, Dance *et al* 2000, 2009, Dance and Sechopoulos 2016, Sarno *et al* 2017a, 2017b,). Standard methods for breast dosimetry also involve the incident air kerma measurement using an ion chamber (Dance and Sechopoulos 2016). Investigation results achieved by Dance (Dance 1990, Dance *et al* 2009), Wu *et al* (Wu *et al* 1994, Sobol and Wu 1997) and Boone (1999, 2002) provided the conversion factors from air kerma to MGD that has been used as reference for dosimetry in mammography. These results are also the basis for algorithms of digital mammography systems that allows in certain level monitoring and reporting of the MGD.

One class of limitations for estimating MGD are related to the inherent uncertainties when it involves experimental procedures, for example, air kerma measurements. It must also be considered the simplifications inherent on computer simulations. Simplifications and non-realistic assumptions of modeling parameters, such as, skin models (Massera and Tomal 2018), breast density (Yaffe *et al* 2009, Boone *et al* 2017), glandular and adipose tissue as a homogeneous mixture (Sechopoulos *et al* 2012, Dance and Sechopoulos 2016) and simple breast models (Hernandez *et al* 2015) impact on glandular dose estimations (Sarno *et al* 2017b).

In a recent review, Dance and Sechopoulos (2016) have pointed out the considerably development of methods for breast dosimetry in mammography. Nevertheless, the authors concluded that further work is still required to improve the modelling and dose estimation processes, to reduce the systematic errors associated with the computational models used for the calculation of the conversion factors which relate air kerma to MGD. Besides the standard breast dosimetry methods, few alternative methods for dose estimation are reported in Dance and Sechopoulos review for mammography. Most of them suggest the use of dosimeters (TLD, OSLD, etc), for example, to measure the air kerma during the imaging procedure (Aznar *et al* 2005, Bastos *et al* 2011) or to measure relative depth dose (Karlsson *et al* 1976, Camargo-Mendoza *et al* 2011). Since it is not feasible to measure the absorbed dose directly into the glandular tissue, the experimental approaches are constrained to use incident or depth dose to estimate the mean glandular dose. Despite this limitation, experimental approaches can be applied for the evaluation of dose in mammography systems and for dose comparison/verification with results from simulation.

The present work reports an alternative experimental method to derive mean glandular dose in clinical mammography devices. This method is based on the difference between the measured x-ray spectra incident and transmitted through breast equivalent materials simulating different glandular/adipose proportions. Depth-dose distributions were also evaluated using both x-ray spectra measured at different depths of breast phantoms and TLDs (TLD-100, Harshaw Chemical Company). This method stands out by using specific experimental spectra from a mammography system instead of ones generated by simulations or theoretical/semi-empirical models. The methodology adopted for spectra measurements and corrections was previously tested and prove to provide an accurate representation of photon energy distribution from x-rays beams in a mammography device (Santos *et al* 2017). Mammography x-ray spectra are commonly obtained from estimations using different methods instead of experimental procedures. Despite this, Hernandez *et al* (2017) pointed out there are only two reported methods focused specifically on mammography x-ray spectra that offer both a range of tube potentials and different target/filter combination. Moreover, parameters impacting x-ray production such as, target composition, effective anode angle, inherent filtration, source-to-detector distance, and focal spot size, may not be the same for different commercially available mammography systems and, in some cases, they are not clearly described when are modeled for spectra generation (Wilkinson *et al* 2001). Therefore, x-ray spectrum measurements overcome these limitations.

Since the most of low-energy photons of mammography beams are attenuated in the first layers of the breast, absorbed dose is nonuniformly distributed within the tissue, with regions close to the entrance beam receiving doses larger than the MGD (Muñoz *et al* 2018). Depth-dose or distribution of normalized glandular dose (depth-DgN_p) are suitable approaches to explore the problem of energy deposition in the breast using tissue-equivalent materials. The use of both TLDs and measured x-ray spectra to evaluate these distributions combines information about the energy spectra hardening due to the photon's interaction processes within the phantom and total depth dose deposition. As the photon energy distributions are known at the TL dosimeter position using this approach, the local dose deposition was measured, providing a complete and accurate description of absorbed dose in these breast phantoms.

2. Material and methods

2.1. X-ray spectra measurements

Mean glandular dose evaluations were performed using x-ray spectra incident and transmitted by phantoms composed by different fractions of breast tissue equivalent materials with glandular/adipose equivalency of 50/50 and 30/70 (CIRS, model 012A[4], Norfolk, USA). The MGD was also evaluated for the 50/50 breast phantom using

[4] Model 012A includes tissue-equivalent breast phantoms and soft tissue-equivalent slabs with different proportion of glandular and adipose material. In this work it was used the tissue-equivalent slabs (BR series) referred as 'phantom'.

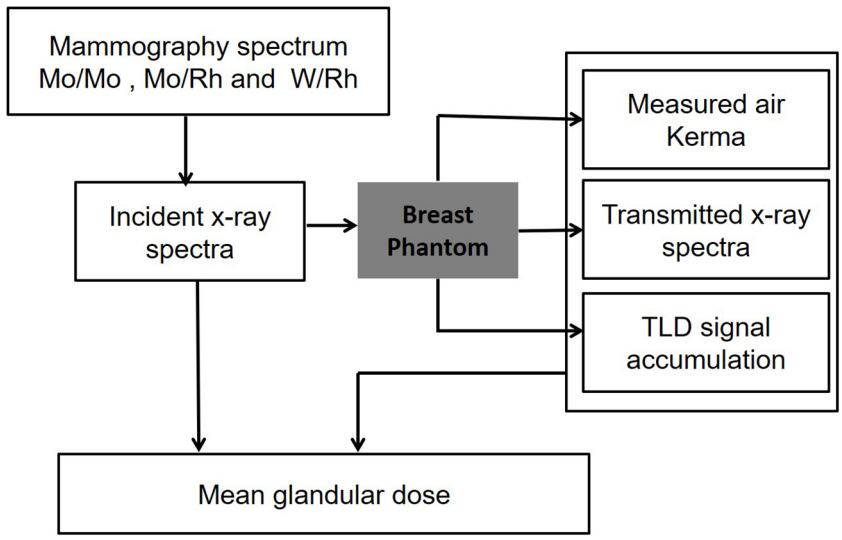

Figure 1. Summary of parameters and experimental setup used for production of incident and transmitted x-ray beam through breast phantoms from which mean glandular dose was derived.

TLDs and compared to the respective results obtained from the measured x-ray spectra for this same phantom. Figure 1 summarizes the sequence of steps and experimental conditions used to data acquisition for the mean glandular dose derivation.

A Siemens Mammomat 3000 Nova system (Siemens AG, Germany) was used to generate the mammographic spectra using three different target/filter combinations (Mo/Mo, Mo/Rh and W/Rh) and the tube potentials of 26 and 28 kVp. These x-rays beams were measured in free air (primary spectra) and after being attenuated by sets of breast-equivalent materials (slab phantoms). Slabs with same composition were combined in order to obtain the thicknesses ranging from 0.5 to 4.5 cm used in the setup for measuring the transmitted x-ray spectra. The decreasing of photon counting rates with the increasing of attenuator thickness requires multiples sequential exposures in order acquire a spectrum with good statistics and it can overheat the mammography tube. This fact limited the maximum phantom thicknesses to 4.5 cm. As a consequence, the tube potentials of 26 and 28 kVp were chosen for being representative of a common technique for imaging breast below than 5 cm (Bushberg *et al* 2011).

The x-ray spectra were measured using a portable spectrometry system model XR-100T with a 9 mm^2 CdTe detector connected to a digital pulse processor model PX4 (Amptek, Inc., Bedford, MA, USA). The detection area was limited by tungsten alloy collimators with diameters varying from 25–100 μm and positioned at 20.5 cm from the breast support. The spectrometer positioning, alignment method and spectra corrections were performed by using the procedures previously described by Santos *et al* (2017). For each measured spectrum, air kerma measurements were performed using a dedicated mammography ionization chamber model 10 × 5—6M (Radcal Corp., Monrovia, CA, USA) properly calibrated by a Secondary Standard Dosimetry Laboratory (SSDL) (IAEA 2007). X-ray spectra corrections were applied for the detector efficiency, Compton distortion and fluorescent escape fraction using the stripping procedure (Di Castro *et al* 1984) as described by Santos *et al* (2016).

Figure 2 depicts the experimental arrangement for the x-ray spectrum measurements. The spectrometer was mounted on the breast support of the mammography system to measure the incident (a) and transmitted x-ray spectra (b). The ionization chamber was mounted at the same position of the CdTe detector for the air kerma measurements (c). The breast phantom was positioned on a plastic support such as a frame contacting only approximately 1 cm phantom's edge. Therefore, it can be considered the measured collimated beam did not interacted with this material. The compression paddle was not used in the setup because of space limitations of the experimental arrangement, but the dose calculation included mathematically the spectra attenuation by 1.4 mm PMMA (used to represent the Mammomat 3000 Nova compression paddle). Linear attenuation coefficients of PMMA from NIST database (Hubbell and Seltzer 2004) were used for calculating the attenuation factor of this material for each energy in the spectrum. All spectra were corrected by these attenuation factors before the dose calculation.

2.2. Mean glandular dose derivation

For a given homogeneous breast-equivalent material with mass, m, simulating a weight fraction of glandular tissue, f_g, and density, ρ, the mean glandular dose can be estimated from the incident, $\phi_0(E)$, and transmitted,

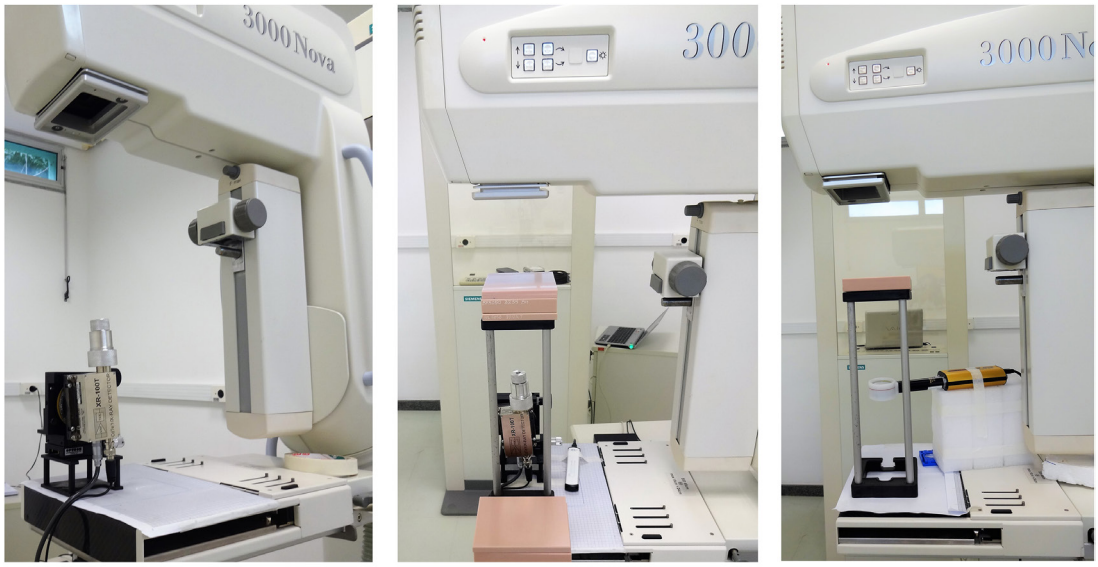

(a) (b) (c)

Figure 2. Experimental arrangement for primary x-ray spectra (a), transmitted x-ray spectra (b) and the air kerma (c) measurements.

$\phi_1(E)$, x-ray spectra through this material. The difference between these spectra represents the fraction of photons that interacted with this material:

$$\phi_{int}\ (E) = \phi_0\,(E) - \phi_1\,(E)\,(\text{photons mm}^{-2}\,\text{keV}^{-1}). \tag{1}$$

The detected x-ray beam is an approximation of the transmitted photons through a cylindrical volume with the base area equal to the exposed detector area and with height, L, as shown in figure 3.

The absorbed dose, in Grays, in the highlighted volume in figure 3 can be calculated by equation (2):

$$D_{abs} = \frac{c}{\rho L}\sum_{E=E_{min}}^{E_{max}} \phi_{int}\,(E)\,E\left(\frac{\mu_{abs}(E)}{\mu(E)}\right)\Delta E\,(\text{Gy}). \tag{2}$$

In equation (2), c is the conversion coefficient for energy in keV to Joule, $c = 1.6021 \times 10^{-16}$ J keV^{-1}, $\phi_{int}\,(E)$ is the photon energy distribution that was removed from the x-ray beam as it passed through the material due to the photon's interactions occurred in the highlighted volume. The factor $\frac{\mu_{abs}(E)}{\mu(E)}$ represents the fraction of the total photon energy deposited in the medium by primary interaction and it is obtained from the ratio of the mass energy-absorption coefficients by the mass attenuation coefficients. It was considered that the energy was locally absorbed, since the CSDA range (continuous slowing down approximation) for electrons in the considered materials is smaller (approximately 16 μm for 30 keV and CIRS 3070 at worst (Berger *et al* 2017)) than the diameter of considered volume of absorption material. Moreover, electronic equilibrium can always be assumed within the mammography range of energy (Carlsson and Dance 1992).

The mean glandular dose, $\bar{D}_g$, is defined as the ratio of the absorbed energy in glandular tissue, $(E_{abs})_g$, to the mass of breast glandular tissue, m_g:

$$\bar{D}_g = \frac{(E_{abs})_g}{m_g}. \tag{3}$$

Boone (1999) proposed a factor, $G(E)$, for estimating the fraction of the total dose that was specifically absorbed by breast glandular component. This factor was used in previous studies (Cunha *et al* 2010, Tomal *et al* 2013, Nosratieh *et al* 2015) for analytical and Monte Carlo calculations of absorbed dose in the breast:

$$G\,(E) = \frac{f_g\left(\frac{\mu_{en}(E)}{\rho}\right)_g}{f_g\left(\frac{\mu_{en}(E)}{\rho}\right)_g + (1-f_g)\left(\frac{\mu_{en}(E)}{\rho}\right)_a}. \tag{4}$$

In equation (4), f_g represents the weight fraction of glandular tissue,$(\mu_{en}(E)/\rho)_g$ represents the mass energy-absorption coefficients for the glandular tissue, and $(\mu_{en}(E)/\rho)_a$ represents the mass energy-absorption coefficients for the adipose tissue. Considering the $G(E)$ factor, the mean glandular dose can be estimated as shown in equation (5):

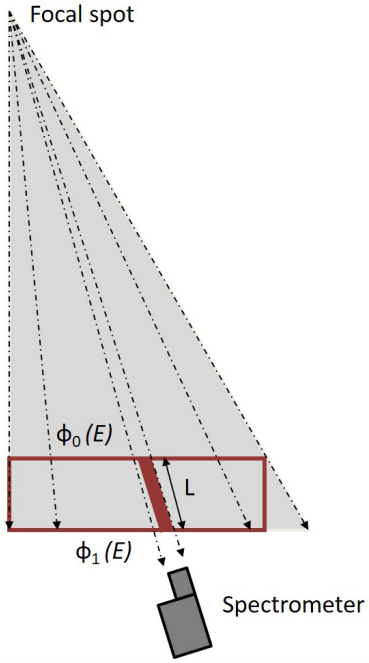

Figure 3. Representation of a breast phantom in a typical mammographic radiation field highlighting the volume of this material that is crossed by the x-ray beam which is detected by a spectrometer. The figure is not in scale.

$$\bar{D}_g = \frac{c}{\rho L f_g} \sum_{E=E_{min}}^{E_{max}} \phi_{abs}\ (E) EG(E)\ (\mathrm{Gy}). \tag{5}$$

Where $\phi_{abs}\ (E) = \phi_{int}\ (E) \left(\frac{\mu_{abs}(E)}{\mu(E)}\right)$ is the absorbed photons distribution in the considered volume. For a measured incident air kerma, K_0, the polyenergetic normalized glandular dose coefficients can be estimated by equation (6):

$$DgN_{\mathrm{p}} = \frac{c}{\rho L f_g K_0} \sum_{E=E_{min}}^{E_{max}} \phi_{abs}\ (E) EG(E)\ \left(\mathrm{Gy\,Gy^{-1}}\right) \tag{6}$$

where the sub index 'p' refers to a polyenergetic x-ray spectrum.

Polyenergetic normalized glandular dose (DgN_{p}) evaluation were performed for breast phantoms with different compositions equivalent to mixtures of glandular and adipose tissues (CIRS30/70, CIRS50/50) using equation (6). The photon energy distribution absorbed by these phantoms, equation (1), was determined from the incident and transmitted x-ray spectra experimentally measured. The absorbed dose (equation (2)) was determined considering the phantom densities estimated by Poletti *et al* (2002). Mass energy-absorption coefficients for the glandular tissue were determined from NIST database (Hubbell and Seltzer 2004) using the composition of this material estimated by Hammerstein *et al* (1979). These coefficients were considered to calculate the $G(E)$ factor, according to equation (4). The proposed method based on x-ray spectra transmitted by the entire material considers only the deposited energy by primary interactions. This approach is reasonable for mammography energy range and small breast and/or phantoms as considered in this work (up to 4.5 cm), but it can cause errors when is applied for higher energies and thicker attenuators, where the contribution of secondary and multiple interactions for energy deposition increase (Wilkinson and Heggie 2000).

Uncertainty of DgN_{p} was considered as a combination of uncertainties in the main variables ρ, L, K_0, E and ϕ_{abs} used to estimate these coefficients (equation (6)). The density values, ρ, of the mammary tissue simulant materials used (CIRS3070 and CIRS5050) and their respective uncertainties were adopted from Poletti *et al* (2002). The maximum uncertainty associated to the phantom thickness was 0.4%. The uncertainty in K_0 is associated to the calibration factor and energy dependency of the ionization chamber used to measure air kerma. The uncertainty in energy (E) is due to the energy spectra calibration and, finally, the uncertainty in ϕ_{abs} represents the spectral counts uncertainties, which are governed by Poisson statistics. Considering the uncertainty sources afore mentioned, the variance of DgN_{p} was calculated by propagation of uncertainty presented in equation (7):

$$\sigma^2_{DgN_{\mathrm{p}}} = \left(\frac{\partial DgN_p}{\partial \rho}\right)^2 \sigma^2_\rho + \left(\frac{\partial DgN_p}{\partial L}\right)^2 \sigma^2_L + \left(\frac{\partial DgN_p}{\partial K_{0,}}\right)^2 \sigma^2_\rho + \left(\frac{\partial DgN_p}{\partial \phi_{abs}}\right)^2 \sigma^2_\psi + \left(\frac{\partial DgN_p}{\partial E}\right)^2 \sigma^2_E. \tag{7}$$

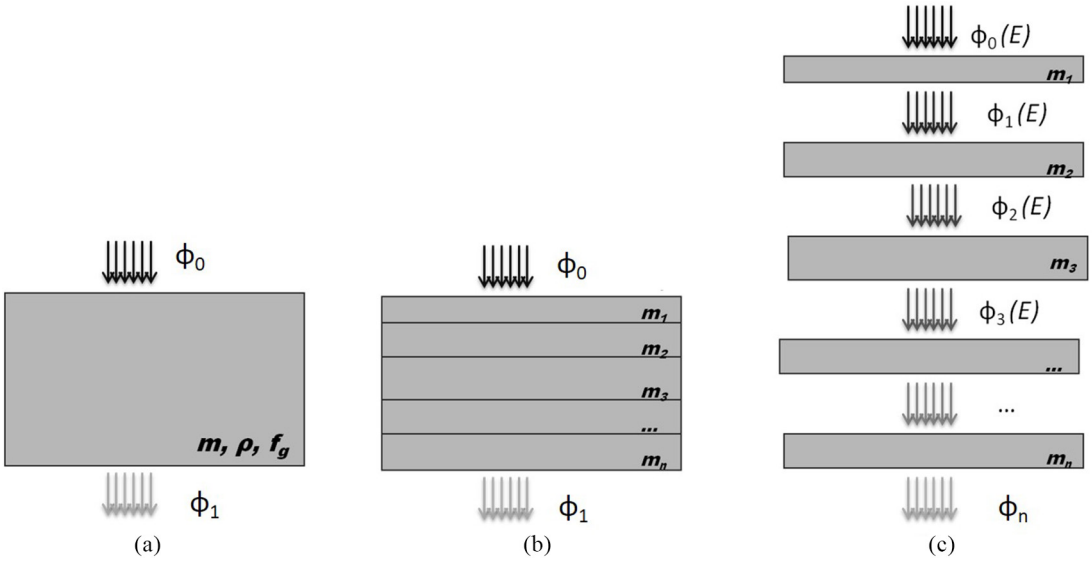

Figure 4. Representation of the x-ray spectra used for the mean glandular dose derivation in a breast phantom (a), the layers considered in this material (b), and the pairs incident-transmitted x-rays spectra in each layer used for the distribution of mean glandular dose derivation (c).

2.3. Polyenergetic normalized glandular dose (DgN_p) distributions from x-ray spectra

The method described in the previous section was applied in two different ways: (i) the DgN_p was calculated considering the incident and transmitted x-ray spectra by the entire material, considering a breast phantom with known thickness; and (ii), the depth-DgN_p distribution in the material was estimated by applying the measured x-ray spectra transmitted by a series of layers of the breast phantom, considering the pair incident-transmitted spectra in each layer. Figure 4 shows a scheme representing the x-ray spectra used for calculating DgN_p (figure 4(a)), the phantoms' layers (figure 4(b)), and the its corresponding incident and transmitted spectra used for calculating depth-DgN_p distributions (figure 4(c)).

The depth-DgN_p distributions were calculated considering the dose deposition in each phantom's layer as presented in figure 4(c). In this case, the value of DgN_p represents the average value of this coefficient of each corresponding layer's thickness, that was 0.5 or 1.0 cm. For exponential fitting purpose in depth-DgN_p data, it was assumed that the DgN_p coefficient obtained in any layer correspond to the DgN_p in the point at the half height of this layer.

Polyenergetic normalized glandular dose was also obtained from the glandular dose in each layer as represented in figure 4(c), by applying equation (8):

$$\bar{D}gN_p = \frac{1}{K_0}\left[\frac{L_1}{L}\,\bar{D}g_1 + \frac{L_2}{L}\,\bar{D}g_2 + \ldots + \frac{L_n}{L}\,\bar{D}g_n\right]. \tag{8}$$

Where L is the thickness of the entire phantom, $L_1, L_2, \ldots, L_n$ are the thicknesses of the layers of the phantom, from the first to the last and $\bar{D}g_1, \bar{D}g_2, \ldots, \bar{D}g_n$ are the mean glandular doses in each layer, from the first to the last one. Since incident and transmitted spectra are known in each layer, $\bar{D}g_1, \bar{D}g_2, \ldots, \bar{D}g_n$ were calculated using equation (5).

2.4. Normalized glandular dose distributions from TLDs

Thermoluminescent dosimeters (TLDs) were also used to evaluate the dose distribution in the breast phantom with glandular/adipose equivalency of 50/50. A set composed by nine Lithium Fluoride doped with Magnesium and Titanium (LiF:Mg,Ti) TLDs (TLD-100, Harshaw Chemical Company, OH, USA) was positioned on the surface of layers of the phantoms (figure 5) and irradiated (using a single exposition) with x-ray beams produced using Mo/Mo, Mo/Rh and W/Rh target/filter combinations, tube voltage of 28 kVp and charge of 100 mAs. The extraction of TLD signal was performed by heating each dosimeter from the room temperature up to 350 °C at a constant rate of 10 °C s^{-1} using a Risø TL/OSL reader model DA-20 (DTU Nutech. Inc., Rolkilde, Denmark). Then, the TLD signal was obtained by integrating the entire thermoluminescence curve. The TLDs were previously free-in-air calibrated using a corresponding standard radiation beam RQR-M2 (at 28 kVp) commonly applied for calibrations of mammography ionization chamber (IAEA 2007). For this procedure, the TLDs were irradiated at different doses measured using a mammography ionization chamber model 10 × 5—6M (Radcal Corp.) and the calibration factor was extracted from the linear curve relating air kerma to TL signal. The group of TLDs selected to be used in this work come from a set of 680 TLDs previously irradiated with

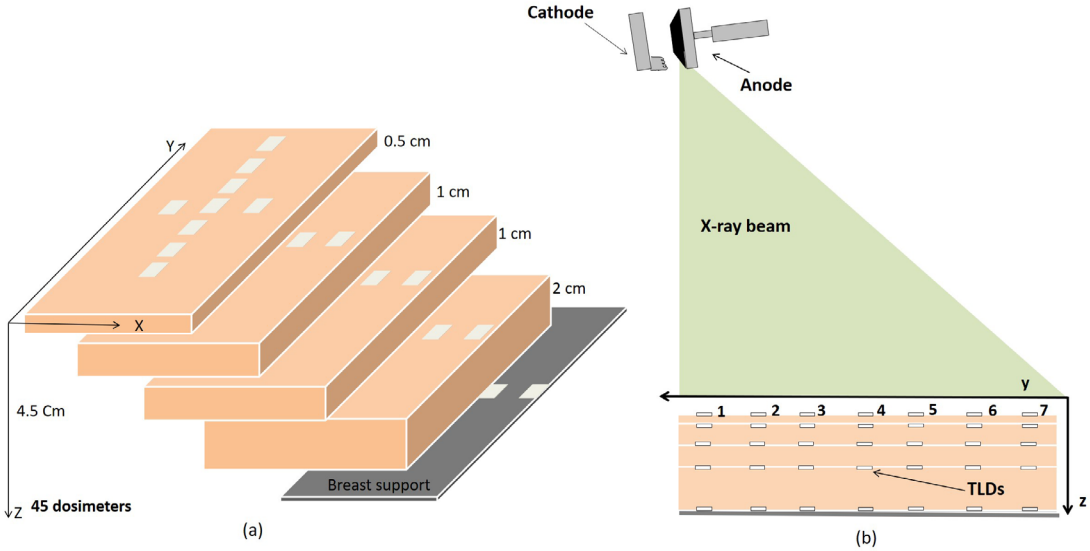

Figure 5. Scheme of the TLDs positioning on the surface of layers of the breast phantom for irradiation using mammography x-ray beams (a). In this scheme, the *y*-axis represents the cathode-anode axis, as presented in the vertical cross section representing the plane yz (b).

2.19 mGy dose using a ^{60}Co source. This selected TLD group presented TL signals within ± 6.5% ($k = 1$) around the average signal of all tested TLDs.

Equation (9) was used to estimate the absorbed dose from TLD readings:

$$D_{phantom}\left(E_{ef}\right) = D_{ar}\left(E_{ef}\right) \frac{\left[\frac{\mu_{ab}}{\rho}\left(E_{ef}\right)\right]_{phantom}}{\left[\frac{\mu_{ab}}{\rho}\left(E_{ef}\right)\right]_{air}}. \tag{9}$$

Where $D_{ar}\left(E_{ef}\right)$ is the absorbed dose in air, calculated from the product of the TL signal and the TLDs calibration factor, and $\left[\frac{\mu_{ab}}{\rho}\left(E_{ef}\right)\right]_{phantom}$ and $\left[\frac{\mu_{ab}}{\rho}\left(E_{ef}\right)\right]_{air}$ are the mass energy-absorption coefficients for the phantom and the air, respectively. The dose in air was not corrected for the variation in response of each dosimeter, but their estimated variations were included in the uncertainty calculation. These coefficients were determined from the data base XCOM provided by *The National Institute of Standards and Technology* (Berger *et al* 2010) considering the beam's effective energy (E_{ef}). The phantom's elementary composition presented by Poletti *et al* (2002) was used to determine these coefficients. Finally, the normalized mean glandular dose was derived from equation (10):

$$DgN = \frac{D_{phantom}\left(E_{ef}\right) G\left(E_{ef}\right)}{K_0} \tag{10}$$

where $G\left(E_{ef}\right)$ is the same function presented in equation(4).

2.5. DgN_p comparisons

2.5.1. *Boone model*

Polyenergetic normalized glandular dose coefficients obtained from equation (6) were compared with results calculated from the model proposed by Boone (2002) and Nosratieh *et al* (2015) and presented in equation (11):

$$DgN_p = \frac{\sum_{E_{\min}}^{E_{\max}} \phi\left(E\right) \vartheta\left(E\right) DgN\left(E\right) \Delta E}{\sum_{E_{\min}}^{E_{\max}} \phi\left(E\right) \vartheta\left(E\right) \Delta E} \tag{11}$$

where $\phi\left(E\right)$ represents the incident polyenergetic photon fluence spectrum, $\vartheta\left(E\right)$ is a function that converts fluence to absorbed dose and $DgN(E)$ are values of normalized glandular dose for monoenergetic beams obtained by Boone using MC Simulation. $\vartheta\left(E\right)$ and $DgN(E)$ are presented in literature (Boone 2002). The spectra $\phi\left(E\right)$ used in equation(11) were the incident x-ray spectra measured as described in item 2.1.

2.5.2. *DgN from DICOM organ dose and Volpara^{TM} software*

DgN_p coefficients obtained in this study from polyenergetic spectra (equation (6)) for breast phantoms with 30% and 50% of glandularity were compared with normalized glandular dose values, DgN, obtained from patient images using both the MGD values reported in the DICOM Organ Dose tag and calculated using Volpara™ software (Volpara Solutions Ltd, Wellington, New Zealand). Raw mammographic images data were analyzed

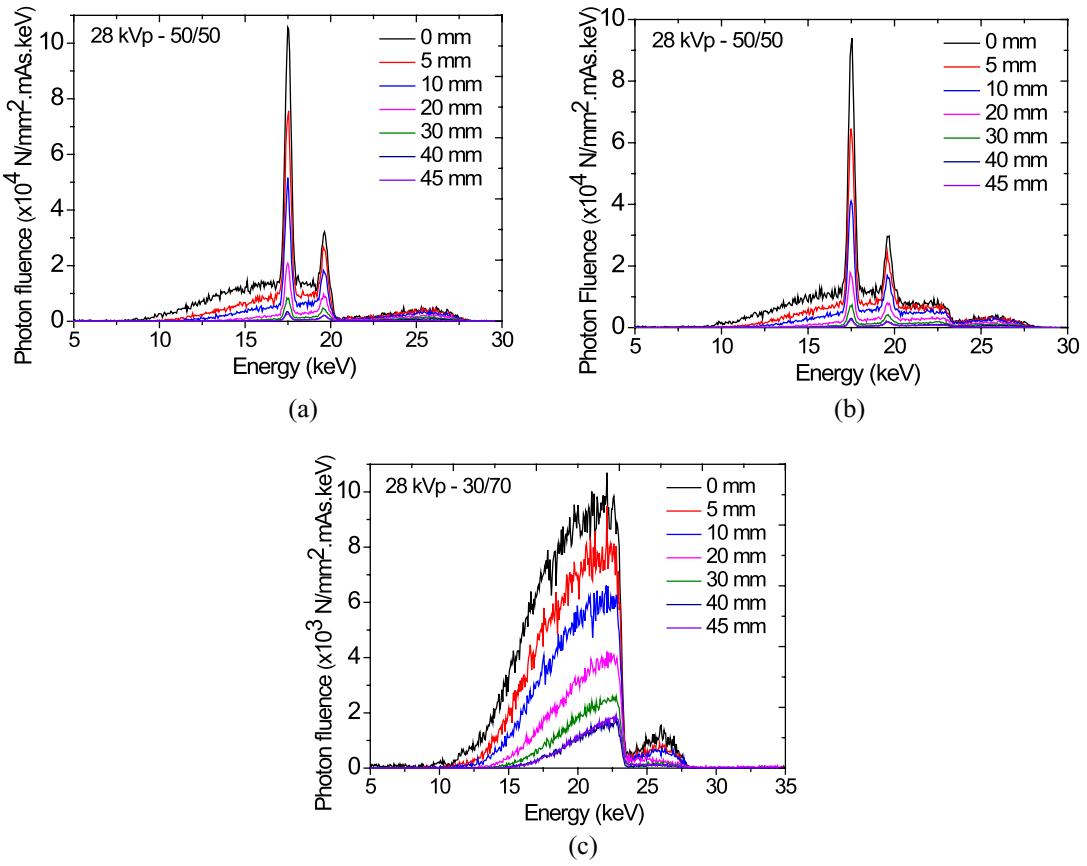

Figure 6. Mo/Mo (a) and Mo/Rh (b) photon fluence spectra incident (0 cm) and transmitted through the phantom CIRS50/50 and W/Rh (c) spectra transmitted by the phantom CIRS30/70. Phantom thicknesses used lies from 0.5 to 4.5 cm. These spectra are normalized by the current-time product (mAs) and are not corrected for the compression paddle attenuation.

using Volpara™ Research 1.5.1 software under a research agreement. Volpara™ is a fully-automated volumetric method for volumetric breast density (VBD) assessment based on the relative physics model (Highnan 2017). A database with more than nine thousand clinical breast images obtained using a Selenia system 2D (Hologic) equipment from the Cancer Institute of the State of São Paulo was used (Tomal 2016). Technical information provided in the DICOM header, such as tube voltage, target/filter combination, compressed breast thickness, MGD, etc, were extracted from the patient images[5]. For each image, the respective values of glandularity and MGD were also calculated by the Volpara™ software. The incident air kerma values recorded in DICOM header were used to normalize both MGD from DICOM header and from Volpara™ calculations.

For the comparison purpose, patient breast images taken using Mo/Mo spectra at 28 kVp with estimated glandularity (by Volpara™ software) of 30% ± 3% and 50% ± 3% were selected. The comparisons of DgN values for breasts with approximately 30% of glandularity involved 58 breast images with recorded breast thicknesses between 3.5–5.5 cm. The comparison of DgN for breast with approximately 50% of glandularity involved 14 breast images with recorded patient's breast thicknesses ranging from 4.2 to 5.8 cm.

3. Results and discussion

3.1. Experimental x-ray spectra

Experimental x-ray spectra from a Mammomat 3000 Nova unit were tested for calculating polyenergetic normalized glandular dose coefficients in breast phantoms. Figure 6 presents some measured photon fluence spectra incident and transmitted through different thicknesses of the phantoms CIRS 30/70 and CIRS 50/50.

The set of spectra presented in figure 6 illustrates the modification of the incident photon energy distribution when the beam is transmitted by different breast phantom thicknesses. The decrease in intensity, especially in low energy regions, with the increasing attenuating material thickness can also be observed. Since the energy deposition on the material depends on photon energy distribution, these spectra can be used for dose estimations.

[5] This study including patient images was previously approved by the local ethical committee (CAAE 47878315.2.0000.5404).

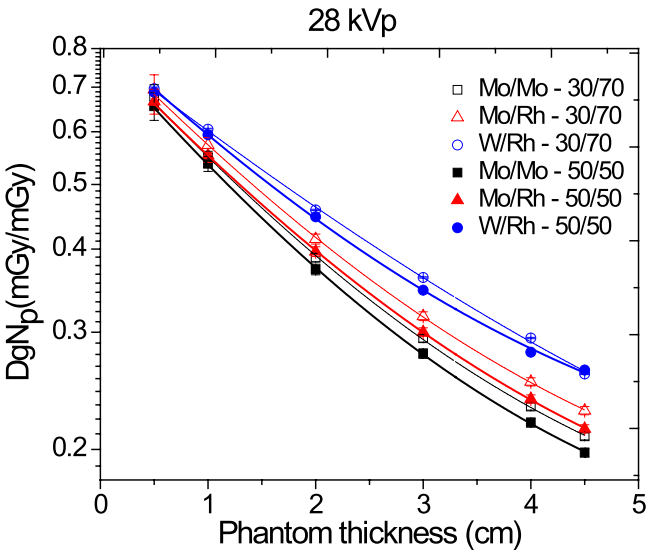

Figure 7. DgN_p values obtained for x-ray spectra generated using the target/filter combination Mo/Mo (black), Mo/Rh (red) and W/Rh (blue) and the tube voltage 28 kVp. The empty symbols represent the results for the phantom CIRS 30/70 and the filled symbols are the results for the phantom CIRS 50/50. The relative expanded uncertainty ($k = 2$) is, on average, 2.6% of the values of DgN_p.

3.2. Polyenergetic normalized glandular dose coefficients (DgN_p)

Figure 7 presents an overview of the DgN_p dependence with the target/filter combination, phantom thickness and density considering a 28 kVp x-ray tube voltage and Mo/Mo (black), Mo/Rh (red) and W/Rh (blue) spectra. The lines are exponential decay fittings. These coefficients (DgN_p) reached the highest values for spectra generated using the W/Rh spectra since this is the target/filter combination that provides x-rays beams with the higher average energy, for the same tube voltage, when compared with Mo/Mo and Mo/Rh target/filter combinations. For the same tube voltage, target/filter combination and material thickness, these coefficients are higher for the material with lower glandularity.

Table 1 presents the DgN_p coefficients obtained for some breast phantoms thicknesses (from 0.5 to 4.5 cm) using the experimental incident and transmitted x-ray spectra such as those presented in figure 6.

Figure 8 compares the DgN_p values obtained using the Boone method (empty symbols), which considers only the incident spectra measured in this work, and the method proposed in the present work.

Results for DgN_p variation with respect to the compressed breast thickness obtained by these two methods as exhibited in figure 8, presented relative difference between 3% and −11% considering the phantom thicknesses of 2, 3 and 4 cm. The observed differences in general were higher to Mo/Rh spectra and 30% of glandularity than to Mo/Mo spectra and 50% of glandularity. Due to the differences in the spectra generation, it is reasonable that the maximum difference between these results is greater than the value of 7% considered as appropriated for comparative dose measurements in diagnostic radiology (IAEA 2007).

Figure 9 presents a comparison between the results of normalized glandular dose for polyenergetic spectra obtained in this work, from equation (6) with results from patient images: DICOM Organ Dose and dose estimation using the Volpara™ software. These results consider Mo/Mo spectrum with 28 kVp and breast compositions of 30/70 (figure 9(a)) and 50/50 (figure 9(b)). Although using a large image database (more than nine thousand mammographic images), for this considered spectrum (Mo/Mo, 28 kVp), few images of breasts with glandularity like that of the phantoms used in this work (30/70 and 50/50) were found: 14 images of breasts with approximately 50% of glandularity and 58 images of breasts with approximately 30% of glandularity. It occurred because the average of breast glandularity in this whole database was (16.9 ± 10.1)%.

Normalized glandular dose values obtained by the three different methods decrease with increasing the breast thickness, as shown in figure 9. DgN coefficients obtained from Volpara considering (30 ± 3)\% glandularity for a 4.5 cm breast thickness are, on average, 8.9% higher than the coefficients for (50 ± 3)% glandularity. A similar difference of 8.5% was observed when the DgNp coefficients obtained in this work for 4.5 cm of the 30/70 and 50/50 breast phantoms were compared. The DgN_p coefficients obtained from the DICOM header for images of 4.5 cm breast with glandularities (estimated using Volpara) of (50 ± 3)% and (30 ± 3)% do not presented significative difference (0.1%). This result is explained if the algorithm for dose estimation of the digital mammography system (Hologic) uses the same glandularity (50%) for the calculation of dose for breasts with different glandularities, such as performed by the Hologic Selenia Dimensions system (Suleiman *et al* 2017).

The values obtained in this work, as described in section 2.2, are close to those obtained from the DICOM header and systematically smaller than the values obtained using the Volpara™ software. It occurs because the

Table 1. Polyenergetic normalized glandular dose coefficients (DgN_p) calculated using x-ray spectra incident and transmitted by some thicknesses of breast phantoms (CIRS 30/70 and CIRS 50/50). These values were obtained from equation (6) for Mo/Mo, Mo/Rh, and W/Rh spectra generated using 26 and 28 kVp. σ_{DgNp} is the relative expanded uncertainty ($k = 2$) and represents, on average, 2.6% of the values of DgN_p.

Tube voltage (kV)	Phantom thickness (cm)	DgN_p (mGy mGy^{-1})	σ_{DgNp} (mGy mGy^{-1})	DgN_p (mGy mGy^{-1})	σ_{DgNp} (mGy mGy^{-1})
		Mo/Mo—30/70		Mo/Mo—50/50	
26	0.5	0.675	0.003	0.619	0.016
	1.0	0.525	0.002	0.518	0.008
	2.0	NC	NC	0.352	0.004
	3.0	0.259	0.001	0.261	0.003
	4.0	0.205	0.001	0.204	0.002
28	0.5	0.678	0.028	0.655	0.031
	1.0	0.549	0.012	0.537	0.014
	2.0	0.388	0.006	0.373	0.007
	3.0	0.294	0.004	0.279	0.005
	4.0	0.232	0.003	0.220	0.003
	4.5	0.209	0.003	0.198	0.003
26		Mo/Rh—30/70		Mo/Rh—50/50	
	0.5	0.674	0.020	0.674	0.016
	1.0	0.550	0.008	0.545	0.007
	2.0	0.394	0.004	0.380	0.003
	3.0	0.300	0.002	0286	0.002
	4.0	0.239	0.002	0.225	0.002
28	0.5	0.694	0.036	0.666	0.029
	1.0	0.573	0.015	0.553	0.013
	2.0	0.414	0.007	0.396	0.007
	3.0	0.317	0.005	0.300	0.004
	4.0	0.253	0.004	0.238	0.003
	4.5	0.229	0.003	0.215	0.003
26		W/Rh—30/70		W/Rh—50/50	
	0.5	0.690	0.006	0.711	0.005
	1.0	0.591	0.003	0.594	0.002
	2.0	0.446	0.001	0.435	0.001
	3.0	0.349	0.001	0.335	0.001
	4.0	0.282	0.001	0.268	0.001
28	0.5	0.696	0.004	0.688	0.004
	1.0	0.605	0.002	0.594	0.002
	2.0	0.458	0.001	0.447	0.001
	3.0	0.363	0.001	0.347	0.001
	4.0	0.294	0.001	0.280	0.001
	4.5	0.260	0.001	0.263	0.001

NC = Not computed.

dose calculation method used in this work and by mammography system Hologic are based on Boone's method (Suleiman *et al* 2017). Average percentage differences between the results presented in figure 9 were evaluated for the breast thickness of 4.5 cm, that is a common thickness between the three methods analyzed. The coefficients DgN_p obtained for the phantom with 30% glandularity are, on average, 8.0% lower than the respective results provided by Volpara™ and 6.4% higher than the results from DICOM Organ Dose. The average percentage differences of the DgN_p values obtained in this work for the phantom with glandularity of 50% with respect to the results obtained from the DICOM headers and Volpara™ software were 2.8% and 7.4%, respectively. DgN_p from Volpara software are, on average, 6.3% higher than DgN_p from DICOM tags when considering the range of breast thicknesses from 4.2 cm to 5.8 cm and glandularity equal to (50 ± 3)%. This difference increases to 15.7% when the glandularity of 30% ± 3% is considered. The increase in this difference for glandularity of 30% occurs because Hologic utilize Boone method for dose estimation (Suleiman *et al* 2017) with the assumption of 50% glandularity. Therefore, a better agreement of DgN from DICOM header when compared to those coefficients

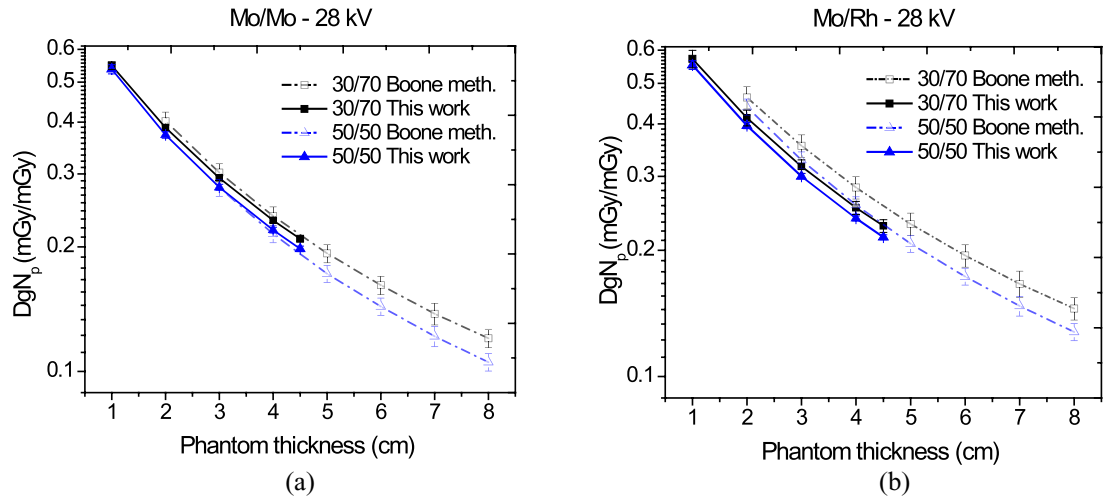

Figure 8. DgN$_p$ obtained by Boone method (empty symbols) and by the proposed method using equation (6) (filled symbols). These results consider (a) Mo/Mo spectra generated with 28 kVp and the glandularity of 30% (black) and 50% (blue), and (b) Mo/Rh spectra generated with 28 kVp and the glandularity of 30% (black) and 50% (blue).

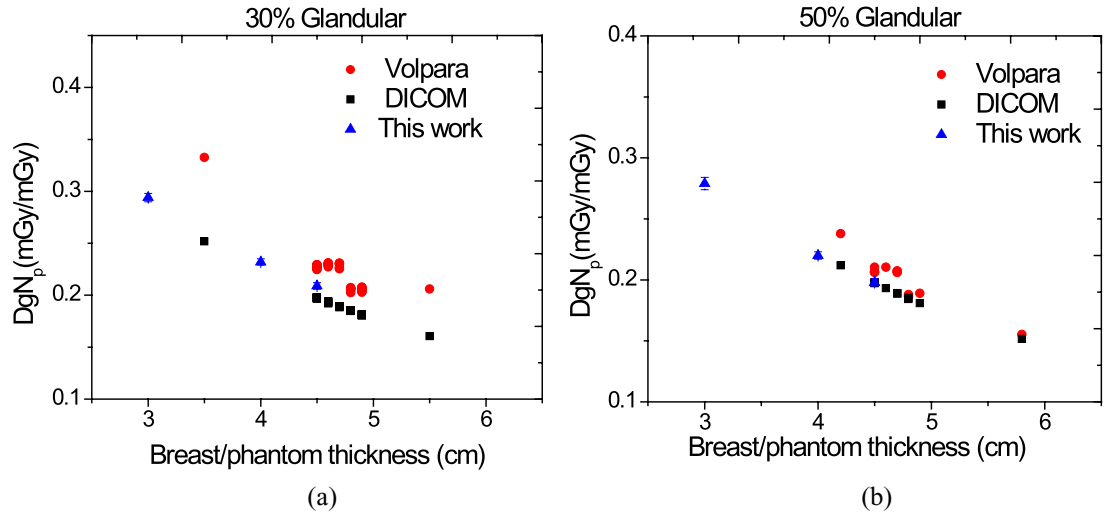

Figure 9. Comparison of polyenergetic normalized glandular dose (DgN$_p$) obtained in this work (equation (6)) from polyenergetic spectra (blue symbols) with DgN coefficients obtained from patient mammograms: using the DICOM Organ Dose (black symbols) and using the Volpara™ software (red symbols) for DgN evaluation. These results consider the Mo/Mo spectra at 28 kVp and breast glandularity of 30%, figure (a), and 50%, figure (b).

from Volpara (with estimated glandularity of (50 ± 3)%) is expected. Results for which DgN values obtained by the Volpara™ software are higher than the values reported by the DICOM Organ Dose had already been observed in the literature (Tromans *et al* 2014, Highnam 2017)

The observed differences between the results from these methods are also due to the different assumption of breast superficial layers in each of the methods. Volpara™ dose calculations assume Dances's model (Dance 1990, Dance *et al* 2000) with a skin and subcutaneous fat layer of 5 mm around the breast. Hologic systems adopt Boone's model (Boone 1999, 2002) for dose estimation with a 4 mm thick skin. The breast phantoms used in this work has no superficial layer to represent the skin. Massera and Tomal (Massera and Tomal 2018) found the DgN differences due to breast superficial layer models with 5 mm adipose and 4 mm skin found by were 16% ± 3%. The difference between the phantom and Dance breast model becomes important at thin compressed breast thicknesses where 1 cm of breast superficial layer (5 mm per side) is significant relative to the total thickness. It can explain the discrepancy observed in figure 9 for thicknesses around 3 cm.

3.3. Polyenergetic normalized glandular dose distributions

Distribution of normalized glandular dose (depth-DgN$_p$ distribution) was estimated in layers at different depths of the breast phantom using experimental x-ray spectra incident and transmitted by each layer as described in section 2.3. It is possible to estimate mean glandular dose in the entire phantom from these distributions. Table 2

Table 2. DgN_p values for layers in different depths of breast phantoms with composition of 30/70 and 50/50. These values were obtained for Mo/Mo, Mo/Rh e W/Rh spectra generated with 26 and 28 kVp. The expanded relative uncertainties ($k = 2$) represent on average 3.6% of the DgN_p values.

Tube voltage (kV)	Depth of the layer (cm)	DgN_p (mGy mGy^{-1})	σ_{DgNp} (mGy mGy^{-1})	DgN_p (mGy mGy^{-1})	σ_{DgNp} (mGy mGy^{-1})
		Mo/Mo—30/70		Mo/Mo—50/50	
26	0.0–0.5	0.675	0.003	0.619	0.016
	0.5–1.0	0.395	0.002	0.429	0.006
	1.0–2.0	NC	NC	0.193	0.001
	1.0–3.0	0.132	0.001	0.084	0.001
	3.0–4.0	0.048	0.001	0.036	0.001
28	0.0–0.5	0.678	0.028	0.655	0.031
	0.5–1.0	0.447	0.020	0.441	0.017
	1.0–2.0	0.237	0.004	0.216	0.004
	2.0–3.0	0.112	0.001	0.097	0.001
	3.0–4.0	0.052	0.001	0.047	0.001
	4.0–4.5	0.033	0.001	0.030	0.001
26		Mo/Rh—30/70		Mo/Rh—50/50	
	0.0–0.5	0.674	0.020	0.674	0.016
	0.5–1.0	0.448	0.017	0.439	0.012
	1.0–2.0	0.250	0.004	0.230	0.002
	1.0–3.0	0.124	0.001	0.107	0.001
	3.0–4.0	0.060	0.001	0.047	0.001
28	0.0–0.5	0.694	0.036	NC	NC
	0.5–1.0	0.477	0.026	0.462	0.013
	1.0–2.0	0.266	0.006	0.250	0.003
	2.0–3.0	0.133	0.002	0.116	0.001
	3.0–4.0	0.067	0.001	0.058	0.001
	4.0–4.5	0.043	0.001	0.033	0.001
26		W/Rh—30/70		W/Rh—50/50	
	0.0–0.5	0.690	0.006	0.711	0.005
	0.5–1.0	0.511	0.005	0.498	0.003
	1.0–2.0	0.314	0.001	0.296	0.001
	1.0–3.0	0.169	0.001	0.147	0.001
	3.0–4.0	0.092	0.001	0.079	0.001
28	0.0–0.5	0.696	0.004	NC	NC
	0.5–1.0	0.531	0.003	0.519	0.003
	1.0–2.0	0.325	0.001	0.312	0.001
	2.0–3.0	0.189	0.004	0.158	0.001
	3.0–4.0	0.099	0.002	0.088	0.001
	4.0–4.5	0.012	0.001	NC	NC

NC = Not computed.

shows the depth-DgN_p distribution obtained for the phantoms with compositions 30/70 and 50/50 in layers ranging from 0.5 to 4.5 cm deep. These values were estimated for Mo/Mo, Mo/Rh and W/Rh spectra generated with 26 kV and 28 kV tube voltages. DgN_p values are higher in the superficial material's layer and decreases to deeper layers. Comparison between DgN_p obtained using the pair incident-transmitted spectra in phantoms with 2, 3, 4 and 4.5 cm thicknesses (from table 1) with DgN_p values derived from the distribution presented in table 2 (using equation (8)) showed differences up to 5.4%. The maxima differences are observed for the Mo/Rh spectra and higher tube voltage, which indicates energy dependence between the results provided by each method.

Figure 10 compares the depth-DgN_p distributions obtained using TLDs and using incident and transmitted x-ray spectra in several phantom layers. The DgN values for TLDs (DgN_{TLD}) in figure 10 were calculated using the average absorbed dose over the TLD readings obtained at each depth and equation (10). The results obtained using TLDs represent the normalized dose in a small volume of $3 \times 3\,mm^2$ area and 1 mm thickness located at a known depth of the material equivalent to breast tissue, whereas the results obtained using x-ray spectra (in

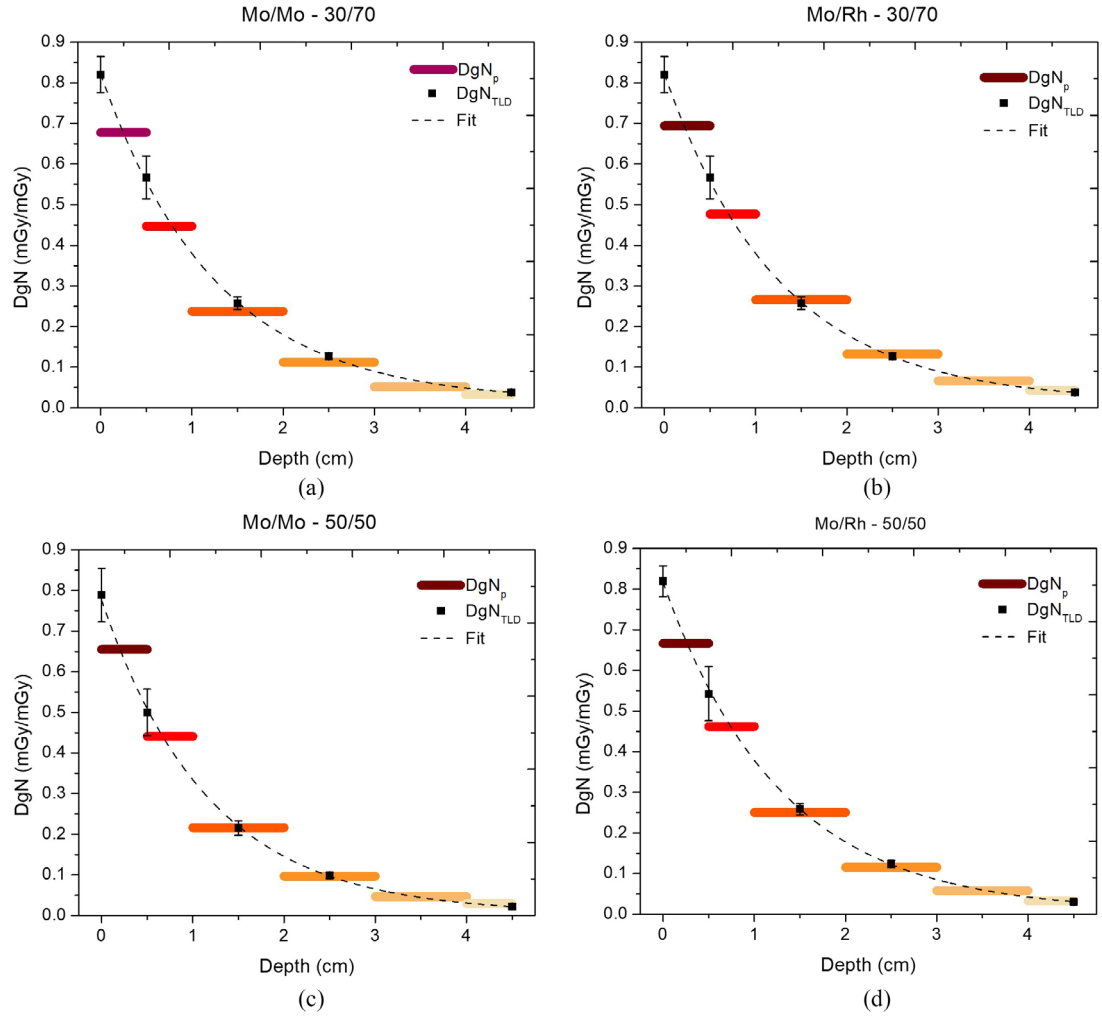

Figure 10. Depth-DgN distributions obtained using TLDs (black symbols) and using x-ray spectra (colored bars). The dotted lines represent an exponential fitting to the data obtained using the TLDs. Results obtained for the breast phantom with composition of 30/70 and Mo/Mo (a) and Mo/Rh (b) spectra. Results obtained for the breast phantom with composition of 50/50 and Mo/Mo (c) and Mo/Rh (d) spectra. All considered spectra in this were generated using 28 kVp.

Table 3. Average values of the normalized glandular dose estimated from the depth-DgN distributions (figure 10) obtained using TLDs, $\overline{DgN}_{TLD}$, and from polyenergetic spectra, $\overline{DgN}_p$. Percentage difference between $\overline{DgN}_{TLD}$ and $\overline{DgN}_p$ with respect to $\overline{DgN}_p$.

X-ray beam—breast phantom	$\overline{DgN}_{TLD}$ (mGy mGy^{-1})	$\overline{DgN}_p$ (mGy mGy^{-1})	Perc. difference (%)
Mo/Mo—30/70	0.236	0.221	1.6
Mo/Rh—30/70	0.260	0.241	1.9
Mo/Mo—50/50	0.202	0.210	- 0.8
Mo/Rh—50/50	0.231	0.227	0.4
W/Rh—50/50	0.302	0.263	3.9

bars) represent the mean dose normalized in layers (0.5 cm or 1 cm) with thicknesses up to 10 times greater than the thickness of the TLDs. According to figure 10, DgN coefficients obtained using TLDs agree to those obtained from x-ray spectra with maximum difference of 3.9%.

Average values of polyenergetic normalized glandular coefficients were calculated over the interval from 0.5 cm to 4.5 cm by means of the DgN obtained for each phantom layer in different depths. The average value of DgN ($\overline{DgN}_{TLD}$ and $\overline{DgN}_p$) was considered as the mean value of an exponential function fitted over the data in figure 10. For purpose of exponential fitting of depth-DgN_p data, it was assumed that the DgN_p obtained in each layer, that is the average value of these coefficients in the respective entire phantom's layer, corresponds to the DgN_p value in a point at the half height of the layer. These data were also extrapolated to the values 0.5 cm and 4.5 cm depth of breast phantom before the exponential fitting. Table 3 presents the average values of the normalized glandular dose estimated from the depth-DgN distributions obtained using TLDs, $\overline{DgN}_{TLD}$ (mGy/mGy), and from polyenergetic spectra, $\overline{DgN}_p$ (mGy/mGy).

According to the data in table 3, DgN coefficients comparison using TLDs ($\overline{DgN}_{TLD}$) and pairs experimental incident-transmitted spectra ($\overline{DgN}_p$) presented maximum percentage difference of 3.9% for the W/Rh spectrum. This difference is acceptable when compared to the maximum uncertainty of 7% considered for comparative dose measurements in diagnostic radiology (IAEA 2007). These results are important for practical applications since it is easier to measure radiation dose using TLD than using spectra. On the other hand, these results also confirm that the proposed method using spectra can be used to estimate glandular dose.

4. Conclusion

Polyenergetic normalized mean glandular dose coefficients were estimated using a method based on the spectral difference in x-ray attenuation of breast phantoms with different composition and thicknesses. Dose distribution inside the breast phantoms and correlations between DgN_p and breast thicknesses, glandularity and target/filter combinations were explored by applying the proposed method.

The procedure of DgN_p derivation for some phantom thicknesses from the DgN_p distributions in depth of these material resulted in DgN_p values that differ not more than 5.2% from the values obtained using only the pairs incident-transmitted spectra in the whole thicknesses considered. The results also showed how dose deposition at the various layers of phantoms depends on the x-ray spectrum used and the influence of the phantom's composition. The variation of the DgN_p with the phantom's depth obtained with TLDs was shown to be consistent with the results observed using the experimental spectra, with maximum difference of 3.9%. For a 4.5 breast phantom and Mo/Mo spectra at 28 kVp, the maximum absolute difference between these coefficients and the respective results from Volpara™ and DICOM Organ Dose were 8.0% and 6.4%, respectively, for glandularity of (30 ± 3)%. A better agreement between DgN from DICOM headers and from Volpara was observed for glandularity of (50 ± 3)% because Hologic systems utilize Boone method for dose estimation (Suleiman *et al* 2017) with the assumption of 50% glandularity.

Despite the complexity in the experimental procedure for mammography spectra measurements, the method for obtaining DgN from measured spectra is innovative and presents consistent results when compared to TLD measurements, reported dose from DICOM images and Boone method. Moreover, the determination of photon energy distributions at certain depths of a breast phantom provides information about the energy spectra modification (hardening) that implies in dose deposition inside the phantom. Finally, it was possible to evaluate the glandular dose in mammography using x-ray spectrometry and the proposed method can be an interesting tool for spectra characterization since it would take into account the variations of each mammography system.

Acknowledgments

The authors thank FAPESP for financial support of the project number 2013/07117-0 and research regular projects 2010/12237-7 and 2015/21873-8, CNPq for support through the projects 312029/2009-8, 483170/2013-5 and 309745/2015-2, and CNPQ/FAPESP funding of the project by INCT—Metrology of Ionizing Radiation in Medicine (grant number 2008/57863-2). They also thank CDTN and ICESP for providing the mammography device for x-ray spectra measurements and the patient images used for dose assessment, respectively. Finally, they thank Dr Ralph Highnam, Dr Ariane Chan and Dr Lisa Johnston from Volpara Solutions Ltd, New Zealand, for providing the Volpara™ Research 1.5.1 software under research agreement and technical support.

References

ACR 1999 *Mammography Quality Control Manual* (Reston, VA: American College of Radiology)

Aznar M C, Hemdal B, Medin J, Marckmann C J, Andersen C E, Bøtter-Jensen L, Andersson I and Mattsson S 2005 *In vivo* absorbed dose measurements in mammography using a new real-time luminescence technique *Br. J. Radiol.* **78** 328–34

Bastos F C, Castro W J, Squair P L, Nogueira M S and Da Silva T A 2011 Feasibility of calibrating thermoluminescent dosimeters in a mammography unit for patient dosimetry *Radiat. Meas.* **46** 2094–6

Berger M J, Coursey J S, Zucker M A and Chang J 2017 ESTAR: Stopping-Power & Range Tables for Electrons, Protons, and Helium Ions (Gaithersburg, MD: National Institute of Standards and Technology) (https://physics.nist.gov/PhysRefData/Star/Text/ESTAR.html) (Accessed: 25 May 2018)

Berger M J, Hubbell J R, Seltzer S M, Chang J, Coursey J S, Sukumar R, Zucker D S and Olsen K 2010 XCOM: Photon Cross Sections Database (version 1.5) (Gaithersburg, MD: National Institute of Standards and Technology) (http://physics.nist.gov/xcom) (Accessed: 25 May 2018)

Boone J M 1999 Glandular breast dose for monoenergetic and high-energy x-ray beams: Monte Carlo assessment *Radiology* **213** 23–37

Boone J M 2002 Normalized glandular dose (DgN) coefficients for arbitrary x-ray spectra in mammography: computer-fit values of Monte Carlo derived data *Med. Phys.* **29** 869–75

Boone J M, Hernandez A M and Seibert J A 2017 Two-dimensional breast dosimetry improved using three-dimensional breast image data *Radiological Physics and Technology* **10** 129–41

Bushberg J T, Seibert J A, Edwin M, Leidholdt J and Boone J M 2011 *The Essential Physics of Medical Imaging* (USA: Lippincott Williams and Wilkins)

Camargo-Mendoza R E, Poletti M E, Costa A M and Caldas L V E 2011 Measurement of some dosimetric parameters for two mammography systems using thermoluminescent dosimetry *Radiat. Meas.* **46** 2086–9
Carlsson G A and Dance D R 1992 Breast absorbed doses in mammography: evaluation of experimental and theoretical approaches *Radiat. Prot. Dosim.* **43** 197–200
Cunha D M, Tomal A and Poletti M E 2010 Evaluation of scatter-to-primary ratio, grid performance and normalized average glandular dose in mammography by Monte Carlo simulation including interference and energy broadening effects *Phys. Med. Biol.* **55** 4335–59
Dance D R 1990 Monte-Carlo calculation of conversion factors for the estimation of mean glandular breast dose *Phys. Med. Biol.* **35** 1211–9
Dance D R and Sechopoulos I 2016 Dosimetry in x-ray-based breast imaging *Phys. Med. Biol.* **61** R271–304
Dance D R, Skinner C L and Alm Carlsson G 1999 Breast dosimetry *Appl. Radiat. Isot.* **50** 185–203
Dance D R, Skinner C L, Young K C, Beckett J R and Kotre C J 2000 Additional factors for the estimation of mean glandular breast dose using the UK mammography dosimetry protocol *Phys. Med. Biol.* **45** 3225
Dance D R, Young K C and Van Engen R E 2009 Further factors for the estimation of mean glandular dose using the United Kingdom, European and IAEA breast dosimetry protocols *Phys. Med. Biol.* **54** 4361–72
Di Castro E, Pani R, Pellegrini R and Bacci C 1984 The use of cadmium telluride detectors for the qualitative analysis of diagnostic x-ray spectra *Phys. Med. Biol.* **29** 1117–31
European Commission (EC) 2013 *European Guidelines for Quality Assurance in Breast Cancer Screening and Diagnosis* (Luxembourg: Office for Official Publications of the European Communities)
Fedon C, Caballo M, Longo R, Trianni A and Sechopoulos I 2018 Internal breast dosimetry in mammography: experimental methods and Monte Carlo validation with a monoenergetic x-ray beam *Med. Phys.* **45** 1724–37
Gennaro G *et al* 2018 Quality controls in digital mammography protocol of the EFOMP Mammo working group *Phys. Med.* **48** 55–64
Hammerstein R G, Miller D W, White D R, Ellen Masterson M, Woodard H Q and Laughlin J S 1979 Absorbed radiation dose in mammography *Radiology* **130** 485–91
Hendrick R E 2010 Radiation doses and cancer risks from breast imaging studies *Radiology* **257** 246–53
Hernandez A M, Seibert J A and Boone J M 2015 Breast dose in mammography is about 30% lower when realistic heterogeneous glandular distributions are considered *Med. Phys.* **42** 6337–48
Hernandez A M, Seibert J A, Nosratieh A and Boone J M 2017 Generation and analysis of clinically relevant breast imaging x-ray spectra *Med. Phys.* **44** 2148–60
Highnam R 2017 VolparaDose White Paper: Patient-Specific Radiation Dose Estimation in Breast Cancer Screening (Wellington, New Zealand: Volpara Solutions) (https://www.volparasolutions.com/assets/ Uploads/VolparaDose-White-Paper.pdf) (Accessed: 14 December 2018)
Hubbell J H and Seltzer S M 2004 Tables of X-Ray Mass Attenuation Coefficients and Mass Energy-Absorption Coefficients (version 1.4) (Gaithersburg, MD: National Institute of Standards and Technology) (http://physics.nist.gov/xaamdi) (Accessed: 17 August 2017)
IAEA 2007 Dosimetry in Diagnostic Radiology: An international Code of Practice *Technical Reports Series* No. 457 (Vienna: International Atomic Energy Agency)
IAEA 2011 *Quality Assurance Programme for Digital Mammography* (Viena: International Atomic Energy Agency)
Karlsson M, Nygren K, Wickman G and Hettinger G 1976 Absorbed dose in mammary radiography *Acta Radiol.* **15** 252–8
Marmot M, Altman D G, Cameron D A, Dewar J A, Thompson S G and Wilcox M 2012 The benefits and harms of breast cancer screening: an independent review *Lancet* **380** 1778–86
Massera R T and Tomal A 2018 Skin models and their impact on mean glandular dose in mammography *Phys. Med.* **51** 38–47
Muñoz I D, Gamboa-deBuen I, Avila O and Brandan M E 2018 Dosimetry in a mammography phantom using TLD-300 dosimeters *Med. Phys.* **45** 4287–96
Njor S, Nyström L, Moss S, Paci E, Broeders M, Segnan N and Lynge E 2012 Breast cancer mortality in mammographic screening in europe: a review of incidence-based mortality studies *J. Med. Screening* **19** 33–41
Nosratieh A, Hernandez A, Shen S Z, Yaffe M J, Seibert J A and Boone J M 2015 Mean glandular dose coefficients (DgN) for x-ray spectra used in contemporary breast imaging systems *Phys. Med. Biol.* **60** 7179–90
Pauwels E K J, Foray N and Bourguignon M H 2016 Breast cancer induced by x-ray mammography screening? a review based on recent understanding of low-dose radiobiology *Med. Princ. Pract.* **25** 101–9
Poletti M E, Gonçalves O D and Mazzaro I 2002 X-ray scattering from human breast tissues and breast-equivalent materials *Phys. Med. Biol.* **47** 47–63
Santos J C, Mariano L, Tomal A and Costa P R 2016 Evaluation of conversion coefficients relating air-kerma to $H*(10)$ using primary and transmitted x-ray spectra in the diagnostic radiology energy range *J. Radiol. Prot.* **36** 117–32
Santos J C, Tomal A, Furquim T A, Fausto A M F, Nogueira M S and Costa P R 2017 Direct measurement of clinical mammographic x-ray spectra using a CdTe spectrometer *Med. Phys.* **44** 3504–11
Sarno A, Dance David R, Engen Ruben E, Young Kenneth C, Russo P, Di Lillo F, Mettivier G, Bliznakova K, Fei B and Sechopoulos I 2017a A Monte Carlo model for mean glandular dose evaluation in spot compression mammography *Med. Phys.* **44** 3848–60
Sarno A, Mettivier G, Di Lillo F and Russo P 2017b A Monte Carlo study of monoenergetic and polyenergetic normalized glandular dose (DgN) coefficients in mammography *Phys. Med. Biol.* **62** 306–25
Sechopoulos I, Bliznakova K, Qin X, Fei B and Feng S S J 2012 Characterization of the homogeneous tissue mixture approximation in breast imaging dosimetry *Med. Phys.* **39** 5050–9
Sobol W T and Wu X 1997 Parametrization of mammography normalized average glandular dose tables *Med. Phys.* **24** 547–54
Suleiman M E, Brennan P C and McEntee M F 2017 Mean glandular dose in digital mammography: a dose calculation method comparison *J. Med. Imaging* **4** 013502
Tomal A 2016 Densidade mamária de mulheres brasileiras *XXI Congresso Brasileiro de Física Médica—Florianópolis* ed J C Santos
Tomal A, Cunha D M and Poletti M E 2013 Optimal x-ray spectra selection in digital mammography: a semi-analytical study *IEEE Trans. Nucl. Sci.* **60** 728–34
Tromans C, Chan A and Highnam R 2014 Comparing personalized mean glandular dose estimates between x-ray systems over time in mammography *European Congress of Radiology*
Wilkinson L E and Heggie J C P 2000 Glandular breast dose: potential errors (electronic letter in response to: Boone J M 1999 Glandular breast dose for monoenergetic and high-energy x-ray beams: Monte Carlo assessment *Radiology* **213** 23–37
Wilkinson L E, Johnston P N and Heggie J C P 2001 A comparison of mammography spectral measurements with spectra produced using several different mathematical models *Phys. Med. Biol.* **46** 1575–89
Wu X, Gingold E L, Barnes G T and Tucker D M 1994 Normalized average glandular dose in molybdenum target-rhodium filter and rhodium target-rhodium filter mammography *Radiology* **193** 83–9
Yaffe M J, Boone J M, Packard N, Alonzo-Proulx O, Huang S Y, Peressotti C L, Al-Mayah A and Brock K 2009 The myth of the 50-50 breast *Med. Phys.* **36** 5437–43